CERAMIC POWER EXTRACTOR DESIGN AT 15.6 GHZ*

A.V. Smirnov, Y. Luo, R. Yi, D. Yu, DULY Research Inc., Rancho Palos Verdes, CA 90275, USA

Abstract

We present here a design of a 15.6-GHz ceramic power extractor. Design features include an upstream parasitic mode damper with additional tapering, and a single-port coupler considered in two variants. Performance analysis includes coupler tolerances and overvoltage, dipole mode wake and BBU, as well as wakefield losses induced in the damper, tapers, and coupler.

INTRODUCTION

A 15.6GHz dielectric power extractor has been designed for high-power testing at the 12th beam harmonic of the upgraded Argonne Wakefield Accelerator (AWA) facility [1]. The 1.3GHz AWA facility upgrade is aimed at producing short (σ_t=2-5ps), intense (q=10-100nC) bunches of energy up to E=19MeV. The extractor design is based on our experience gained from a previous 21GHz design [2] tested in CERN [3]. New design features [4] include the following: single-port outcoupling, high harmonic (12th) of the drive beam, evanescent outlet beam pipe (*i.e.* no choke), symmetrized coupler, longer tapering of dielectric matching section, a short step-like stopper downstream the dielectric tube, and a parasitic mode damper upstream the slow-wave structure.

The steady-state output rf power can be calculated as follows:

$$P = \frac{\omega}{4}\frac{r}{Q}\frac{1}{|v_{gr}|}\left| I\,\Phi_b L\frac{1-e^{-\alpha L.(1+ia_s)}}{\alpha L(1+ia_s)}\right|^2, \qquad (1)$$

where r is the shunt impedance per unit length,

$$\Phi_b = \frac{1}{q}\int_q \frac{dq}{dz}(z')\exp\left(-i\frac{kz'}{\beta}\left(1-\frac{i/2Q}{1-\beta_{gr}/\beta}\right)\right)dz'$$

is the bunch formfactor, $a_s = 2Q(f/n_h f_b - 1)(1-\beta_{gr}/\beta)$ is the generalized detuning, $\omega = 2\pi f = h(\omega)/v$, f_b is the driving linac frequency, $n_h = Integer(f/f_b)$ is the harmonic number, $\alpha = \pi f Q/v_{gr}$, and $2Q|\beta-\beta_{gr}| >> 1$, $\left[L(\beta_{gr}^{-1}-\beta^{-1})f_b/c\right]^2 >> 1$.

The structure is capable of generating P=148MW power in a multi-bunch mode (at σ_t=10ps, q=40nC), and P=77MW in a single-bunch mode (at q=100nC). Because of rapid decrease of the power P and formfactor Φ_b at higher harmonics, the 12th harmonic operation is close to the limit of operational efficiency ($|\Phi_b|$=0.62 for σ_t=10ps).

DIELECTRIC TUBE

The dielectric tube is made of Forsterite ceramics with a dielectric constant ε=6.64, which is low compared to alumina (~10) or magnesium calcium titanate ceramics (~20). Lower ε allows attaining higher r/Q at a given frequency and aperture. It simplifies the extractor/outcoupler design by avoidance of ceramic OD

tapering [5], and reduces overvoltage between ceramic subsections. The ceramics parameters were calculated analytically for an aperture ID of 12mm. Agreement with Gd1 code [6] simulation is within 0.13% for the resonant frequency, and better than 1.1% for the Q-factor.

For downstream matching, different methods of ceramic ID tapering were analyzed using the CST Microwave Studio code [7]: single-step, two-step and conic (linear) tapering. Final optimizations of the downstream linear tapering (21mm length) and the small triangular stopper (Δr=0.25mm=ΔL) were done with the Gd1 code [6]. Results indicate insignificant reflections (S_{11}=-32dB at 15.6GHz) and acceptable overvoltage at the ceramic edges.

Beam dynamics analysis [8] includes beam loading, beam transport and transverse stability. Kinetic energy loss of the last bunch of a 16-bunch train is ~3.2MeV in the AWA linac, which is comparable to that in the dielectric tube (5MeV at σ_t=10ps, 40nC/bunch).

Analytical modeling of the generated waveform is given in Fig. 1. Neglecting jitter and reflections, the signal bandwidth is about 0.33GHz at 10% of the main peak.
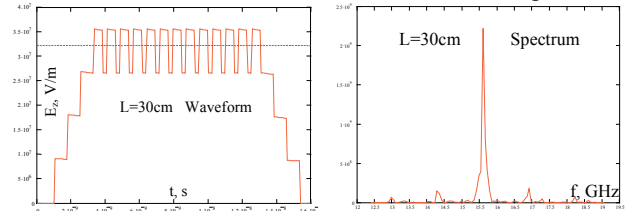

Figure 1: RF envelope of the longitudinal field and its spectrum. δ_z=3mm, q=40nC, N_b=16 bunches. The horizontal dashed line corresponds to the formula (1).

BBU consideration revealed high likelihood of instability in terms of low threshold current ($I_{thr}\approx$12A at q=40nC) and high increment (~0.15GHz) at E=15MeV. The estimations are also consistent with indications observed earlier during the 21GHz tests [8].

Thus for the planned experiment, a dielectric length of L=30cm is a compromise between reasonable power and spectrum, on the one hand; and adverse transverse beam dynamics, on the other [8].

A parasitic mode damper was designed at the upstream end of the dielectric tube. It prevents build-up of regenerative transverse instability that may occur as a result of high reflections from both ends of the slow-wave structure. The absorber decreases the loaded Q-factor of the dipole mode more than threefold, by reduction of the upstream reflection coefficient Γ_1 by an order (down to ~0.05). Note, the resonant parasitic hybrid modes (14.2 GHz for the TEM$_{11}$ mode and 16.0 GHz for the TEM$_{21}$ mode) have higher group velocities (0.434c for dipole and

0.282c for quadrupole) than that for the fundamental mode (0.26c). The damper (see Fig. 2) may also reduce overvoltage caused by mismatching of the fundamental TM_{01} TW mode.
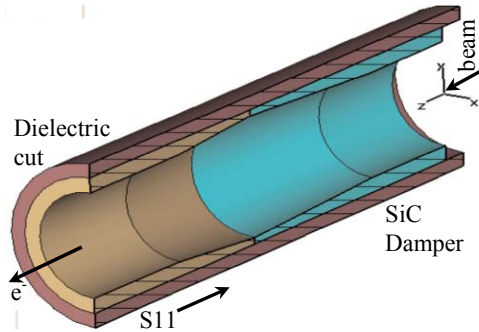

Figure 2: SiC damper (on the right end) for reflected parasitic waves as seen from the regular ceramic tube. S_{11}= -27dB at resonant dipole mode frequency 14.2GHz.

Wakefield energy losses induced by the damper and adiabatic tapers were calculated. The bunches radiate here independently, in a rather wide frequency range, without space-time build-up of the field, because: i) drain time for the damper and tapers is much less than the inter-bunch interval, ii) low Q-factor of the damper reduces dramatically the wake attenuation length $\lambda Q |\beta - \beta_{gr}| / \pi$, iii) tapering and strong attenuation result in decoherence. Under these conditions a simple formula (2) can be used to estimate the energy loss per bunch in these elements:

$$\Delta W_{1b} = \frac{q^2}{4} \int_{z_1}^{z_2} \frac{\omega(z) r(z)}{Q(z)} \cdot \frac{|\Phi_b(z)|^2}{1 - \beta_{gr}(z)/\beta} dz \,, \qquad (2)$$

where $z_2 - z_1 \gg \delta_z$, and $\omega, r/Q, \beta_{gr}, \Phi_b$ are defined analytically from eigenmode problem solved at different cross-sections of the tapered element. For q=40nC, δ_z=3mm bunch(es) it gives ~0.05MeV kinetic energy loss for the damper and ~0.09MeV for the tapers on both ends of the regular dielectric radiator.

Completely analytical modeling is also effective for estimating tolerances in terms of decrease of power (<10% at saturation) and single bunch spectrum broadening of <20% (assuming the length of the regular tube is 30cm). We found ~.001 inch for the ceramic cylinder radii and 1% for the dielectric constant to be satisfactory.

To close any gaps between ceramic subsections, a spring in compression is placed upstream the damper along with a stopper downstream the dielectric tube (see the mechanical design in Fig. 8). Open gaps as large as 20-150µm would otherwise result in considerable overvoltage [4,5] proportional to the dielectric constant.

SINGLE-PORT OUTCOUPLER

The coupler design is dominated by three issues: i) The radius of the copper pipe loaded by dielectric (outer radius =7.71mm) is near the cutoff (7.36mm), ii) The evanescent outlet beam pipe has a relatively large radius (6mm), iii) The short-pulse, sub-harmonically driven source has a substantial bandwidth. Different configurations of the coupler were simulated and optimized: (i) asymmetrical, (ii) symmetrized with one or two shorting stubs loaded with tapered cylinder, (iii) pillbox symmetrized with four rods. Optimized designs shown in Fig. 3 have both good transmission >0.99 (see Fig. 4) and bandwidth (~1GHz – about triple the main peak width of Fig. 1). The coupler parameters are summarized in Table 1.
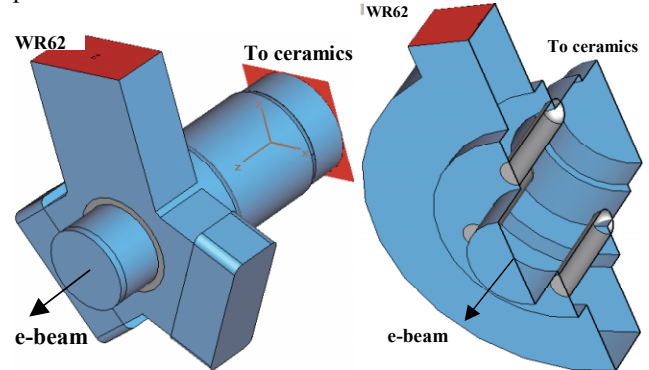

Figure 3: Two-stub (on the left) and four-rod (on the right, one half) couplers designed with the MWS code.
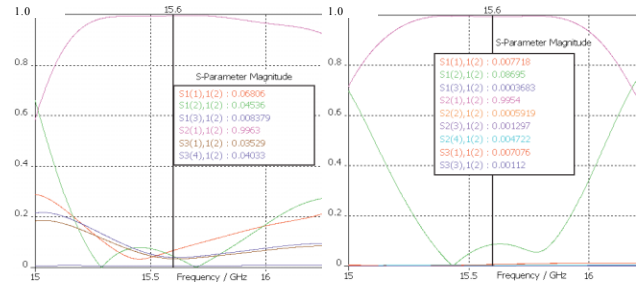

Figure 4: S-parameters for the two-stub coupler (on the left) and four-rod coupler (on the right). Transmission coefficient is $S_{21} \equiv S2(1)1(2)$.

Table 1: Comparison of the Two Designs of the Coupler

Parameters \ Design	2 stubs	4 rods
S_{21} @ 15.6GHz	0.996	0.995
Bandwidth @ S_{21}=0.9, %	5.63	5.79
S1(1)1(2) @ 15.6GHz	0.068	0.0077
Min. coupler length, mm	28.4	20.6
Max. overvoltage factor	4.13	2.12
RMS tol. @Bandwidth=4.5%	42µm	17µm
RMS tol. @ S_{21}=0.97	25µm	24µm
Trapped monopole mode	8.1 GHz	No TM_{0mn}

The four-rod design is shorter, produces twice as less overvoltage, and has no trapped modes interacting with the beam. The rods act effectively as a symmetric modal filter. It suppresses by an order parasitic signal seeding instability driven by TM_{01} conversion into dipole (S1(1)1(2)) and quadrupole (S1(3)1(2)) modes.

Sensitivities of the transmission and bandwidth to ±0.001" dimensional variations, performed one-by-one, are depicted in Fig. 5. As expected, both designs are extremely sensitive to the copper tube radius ($rtube$ in Fig. 5), connecting the coupler and the ceramic-loaded

section. In addition, the 4-rod design is very sensitive to the rod position and dimensions. By contrast, the distribution of tolerances is more uniform for the 2-stub design, whereas the fabrication accuracy requirements for the advanced 4-rod design are extremely high.
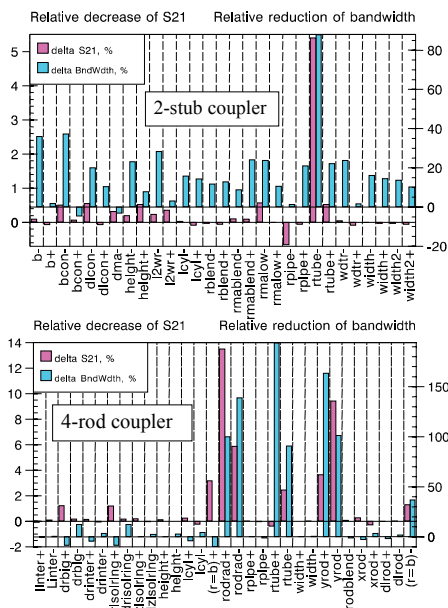

Figure 5: Relative reduction [%] of the transmission (left ordinate) and bandwidth (right) for the two coupler designs *vs* one-by-one dimensional variations (±25.4μm).

Study of trapped modes revealed a TM_{010}-type mode induced in the 2-stub coupler at 8.1GHz. Due to high symmetry of the mode and non-resonant ratio (6.23) to the linac frequency (1.3GHz), this mode does not affect extractor performance and the kinetic energy loss averaged over train does not exceed 0.1MeV [8].
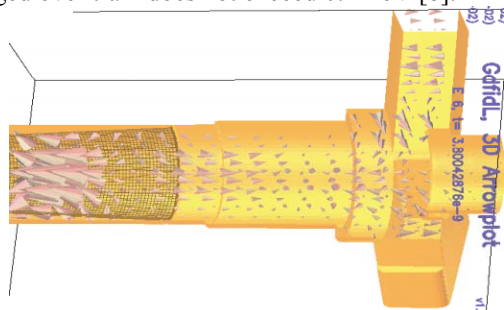

Figure 6: Half model of part of extractor with taper and 2-stub coupler. The fields are induced by a single δ_z=3mm bunch in a short (3cm) regular dielectric.

Single-bunch wakefield induced and propagating in $1/10^{th}$ of the extractor length was simulated up to the WR62 port (see Figs. 6,7). Two satellite peaks can be seen in the signal spectrum of Fig. 7. The first one, the TM_{010}, ~8.1GHz eigenmode of the 2-stub coupler, is evanescent in all 3 ports. Another peak is not a trapped mode. It is produced at first as a wide-band (16.5-35GHz) radiation at the taper, and then filtered by the coupler having a narrow passband near 19.5GHz.

The mechanical design of the entire extractor assembly is shown in Fig. 8.
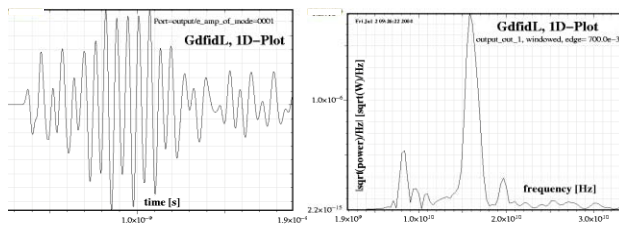

Figure 7: Signal and its spectrum induced in the output port of the 2-stub coupler by the 3mm, 100nC bunch passed through 3cm regular dielectric, tapering and coupler.
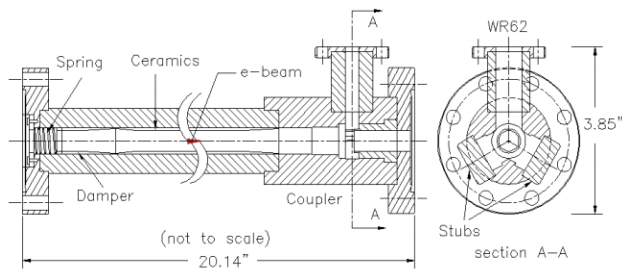

Figure 8: Assembly drawing of the 15.6GHz power extractor with a 2-stub coupler design.

ACKNOWLEDGEMENTS

REFERENCES

[1] M. E. Conde, S. Antipov, W. Gai, C. Jing, R. Konecny, W. Liu, J. G. Power, H. Wang, Z. Yusof, in AIP Conf. Proc., v. 737 (2004) 657.

[2] D. Yu, D. Newsham, A. Smirnov, Proc. 10th Adv. Accelerator Workshop, AIP 547, pp. 484-505, 2002.

[3] D. Newsham, A. Smirnov, D. Yu, W. Gai, R. Konecny, W. Liu, H. Braun, G. Carron, S. Doebert, L. Thorndahl, I. Wilson, W. Wuensch, in Proc. of 2003 Part. Acc. Conf., Portland, Oregon, May 12-16 (2003) 1156.

[4] A.V. Smirnov, Y. Luo, D. Yu, in AIP Conf. Proc., v. 737 (2004) 971.

[5] C. Jing, R. Konecny, W. Gai, S.H. Gold, J.G. Power, A.K. Kinkead, W. Liu, in AIP Conf. Proc., v. 737 (2004) 258.

[6] Warner Bruns, GdfidL v. 1.8: Syntax and Semantics, March 13, 2002; http://www.gdfidl.de.

[7] High Frequency Electromagnetic Software, version 5, Sonnet Software Inc.

[8] A.V. Smirnov, D.Yu, W.Gai, H.Wang, in AIP Conf. Proc., v. 737 (2004) 914.